Solid State Sciences 20 (2013) 110–114

Contents lists available at SciVerse ScienceDirect

Solid State Sciences

journal homepage: www.elsevier.com/locate/ssscie

Performance improvement on $LiFePO_4$/C composite cathode for lithium-ion batteries

Ondrej Cech [a], Jorge E. Thomas [b], Marie Sedlarikova [a], Andrea Fedorkova [a,c,*], Jiri Vondrak [a], Mario Sergio Moreno [d], Arnaldo Visintin [b]

[a] Department of Electrical and Electronic Technology, Faculty of Electrical Engineering and Communication, Brno University of Technology, Technicka 10, 616 00 Brno, Czech Republic
[b] Instituto de Investigaciones Fisicoquímicas Teóricas y Aplicadas (INIFTA), Fac. de, Ciencias Exactas, UNLP, CCT La Plata-CONICET, C.C. 16, Suc. 4, CP 1900 La Plata, Argentina
[c] Institute of Chemistry, Faculty of Science, P.J. Šafárik University, Moyzesova 11, SK-041 54 Košice, Slovak Republic
[d] Centro Atómico Bariloche, Comisión Nacional de Energía Atómica (CAB-CNEA), (8400) S.C. de Bariloche, Argentina

ARTICLE INFO

Article history:
Received 24 October 2012
Received in revised form
7 March 2013
Accepted 19 March 2013
Available online 2 April 2013

Keywords:
Lithium-ion battery
Phosphate
Cathode
$LiFePO_4$
Cobalt

ABSTRACT

Temperature glycine assisted solid-state synthesis was used to prepare $LiFePO_4$/C composite samples with two types of material improvements. It will be shown how can addition of a high conductive support as well as doping with supervalent metal ions improve the electrochemical performance of Li-ion cathode. Three samples with different properties were prepared and investigated – pure $LiFePO_4$/C with no material improvements, $LiFePO_4$/C prepared with multi walled carbon nanotubes (MWCNT) conductive support and $LiFePO_4$/C doped by 1% of cobalt. Glycine was used as inorganic carbon coating precursor during the synthesis of all samples. XRD measurements confirmed production of highly crystalline $LiFePO_4$ cathode material with diameter varying between 40 nm and 200 nm. Electrochemical measurements confirmed increasing the intra-particle conductivity by MWCNT or Co doping. Galvanostatic battery testing shows that $LiFePO_4$/MWCNT/C composite delivers highest capacity 130 mA h g^{-1} at C/5. $LiFePO_4$/MWCNT/C cathode material prepared by solid state synthesis exhibit excellent electrochemical performances, improved conductivity, and good rate capability compared to the $LiFePO_4$/C composite material.

1. Introduction

Nowadays, lithium-ion batteries are key components in a lot of everyday use of electronic equipment like mobile phones, computers and other portable devices. The need of stable, safe and high power density energy sources is rapidly growing with hybrid and electric vehicle market expansion. Active cathode and anode materials are the host compounds for cyclic lithium insertion and extraction. Since the first lithium-ion batteries were developed, more structural types of active materials were proposed. First intercalation compounds were the layered-structure rock salt oxides $LiCoO_2$ and $LiNiO_2$ and subsequently the spinel $LiMn_2O_4$ [1]. All the above mentioned materials are still widely commercially used even for middle-power applications. The main problem of these conventional materials is poor chemical and electrochemical stability in their highly oxidized state [2]. Among several components in the lithium ion batteries, cathode materials have attracted much attention in recent years [3]. Introduced in 1997 by Padhi et al., olivine structured $LiFePO_4$ has emerged as one of the most promising cathode materials for the next generation of lithium ion batteries [3]. $LiFePO_4$ is highly interesting as it is relatively inexpensive and environmentally benign [4]. $LiFePO_4$ has a high theoretical capacity of about 168 mA h g^{-1}, flat discharge plateau at 3.4 V vs. Li/Li^+, long cycle life due to a small volume change (6.8%), and very good cycling stability. On the other hand, there is an intrinsic electron conductivity of bulk material as low as 10^{-9} S $cm^{-1}$and poor ionic conductivity 10^{-5} S cm^{-1} [5]. There are some basic approaches to dealing with the low conductivity problems. Syntheses producing nanostructured particles of active material are used for better active mass utilization [6–8]. Electronic conductivity can be increased by mixing active material with conductive supports, and especially by coating active material particles with highly conductive materials like carbon from organic precursors [8–11] or conductive polymers. Ionic conductivity can be improved by supervalent metal ion doping or substitution and by producing a nanoporous network [8]. Carbon coating or metal/

* Corresponding author. Department of Electrical and Electronic Technology, Faculty of Electrical Engineering and Communication, Brno University of Technology, Technicka 10, 616 00 Brno, Czech Republic. Tel.: +421552342328.
E-mail address: andrea.fedorkova@upjs.sk (A. Fedorkova).

1293-2558/$ – see front matter © 2013 Elsevier Masson SAS. All rights reserved.
http://dx.doi.org/10.1016/j.solidstatesciences.2013.03.017

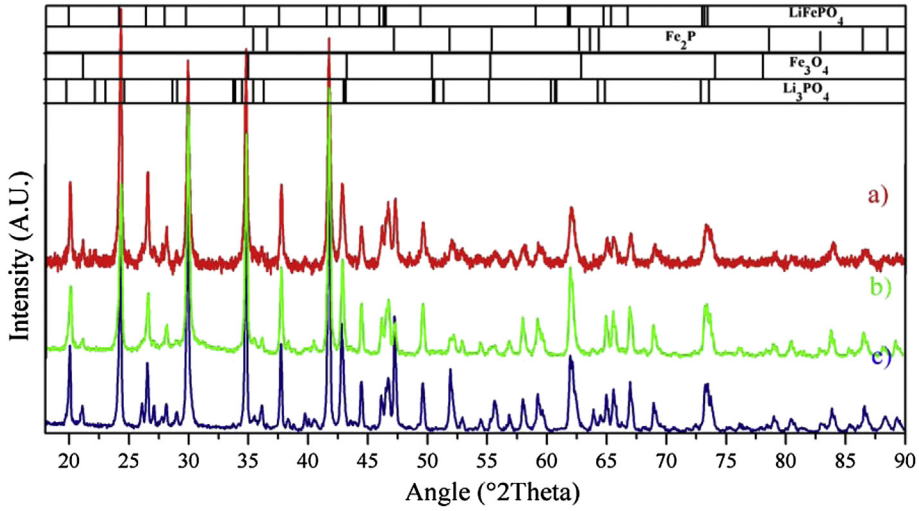

Fig. 1. XRD patterns of the $LiFePO_4$/C composites a) pure $LiFePO_4$/C, b) $LiFePO_4$/MWCNT/C, c) cobalt doped $LiFePO_4$/C with impurities indicated at the top of picture.

metal oxide coating can enhance the conductivity between particles, but has a little effect on the internal conductivity of $LiFePO_4$. When the $LiFePO_4$ particles are not small enough (30–200 nm), it is difficult to get a high-rate charge and discharge performance. Therefore, increasing the intra-particle conductivity by multi walled carbon nanotubes (MWCNT) or Co doping is a very important issue. Apart from the afore mentioned approaches, metal ion doping in the Li or Fe site is regarded as a promising method for increasing electrical conductivity and working voltage [12]. Cobalt [13,14], manganese [15], nickel [16], and vanadium [17] are considered favourable dopants because of the higher chemical potential of $Co^{2+/3+}$, $Mn^{2+/3+}$, $Ni^{2+/3+}$, and $V^{2+/3+}$. Herein, we report a facile solid state approach for the synthesis of $LiFePO_4$ cathode material exhibiting good electrochemical properties after doping with cobalt or mixing with MWCNT.

2. Experimental

2.1. Preparation of samples

For the material preparations, the glycine assisted combustion method was used as published elsewhere [8] and slightly modified. A stoichiometric amounts of lithium nitrate (0.9 g, Sigma–Aldrich), iron oxalate (2.4 g, Sigma–Aldrich) and ammonium dihydrogen phosphate (1.7 g, Sigma–Aldrich) were dissolved in 10 ml of deionized water, heated to 60 °C and stirred until a homogenous solution was obtained. Another solution prepared by dissolving 2 g of glycine (Sigma–Aldrich) in 10 ml of hot deionized water (90 °C) was poured into it. The molar ratio of glycine to $LiFePO_4$ was 2:1, 2 wt.% of carbon conductive support (Timcal Super P or MWCNT with diameter 3–10 nm, length 10–20 μm) was added to the hot solution and the resulting mixture was heated up to 95 °C and continuously stirred until a creamy mass was obtained. In case of cobalt doped sample, 1 wt.% of cobalt in ratio to resulting $LiFePO_4$ was introduced to the solution in the form of 0.1 g cobalt nitrate hexahydrate. The prepared product was collected, put onto a stainless steel plate in a tube furnace and dried in flowing argon atmosphere at 300 °C for 12 h. Finally, the cathode material was sintered at 750 °C for 6 h in flowing Ar atmosphere to prevent the oxidation process. When removed from the furnace, the material was milled in a ball mill and the powder thus obtained was used for physical and electrochemical characterization.

The slurry was made by mixing the active cathode material with Super P carbon and polyvinylidene fluoride (PVdF) in *N*-methyl-2-pyrrolidon (NMP) with a weight ratio of 80:10:10. This paste was then coated onto aluminium foil as current collector using the doctor-blade technique and subsequently dried in a vacuum oven at 130 °C for 18 h. Circular electrodes with 18 mm diameter were cut out of the coated foil, with an area of 2.54 cm^2 and total mass of 2.2–2.6 mg on a substrate of Al foil. Test cells were assembled using these cathodes with a counter and a reference electrode made from lithium metal foil and a separator layer (SEPARION® and fiber glass separator Whatman GF/D). All handling was done in an argon filled dry glove box. The electrolyte consisted of 1 M $LiPF_6$ in ethylene carbonate/ethylmethyl carbonate (EC/EMC, volume ratio 1:1).

2.2. Electrochemical testing

Cyclic voltammetry (CV) measurements were performed at room temperature using a three-neck glass tube cell placed in Ar filled glovebox. For charge–discharge cycling, rate capability and electrochemical impedance spectroscopy measurements (EIS), the two electrode El-Cell© coin-type cell was used. Impedance measurements were carried out in the frequency range 10^5 Hz to 0.1 Hz with amplitudes of ±10 mV at room temperature. Cycling measurements were controlled with an Autolab instrument system and performed between 2.5 and 4.0 V vs. Li^+/Li at room temperature.

2.3. Support characterization

The X-ray diffractogram was collected by a Bruker D8 Advance diffractometer equipped with a Göbel mirror and a Cu Kα radiation tube ($\lambda = 0.15406$ nm). TEM evaluations were performed in a JEOL JEM-2000 EX II.

Table 1
Lattice parameters of $LiFePO_4$ deduced from the analysis of X-ray diffraction pattern of our samples.

Sample	*a* (Å)	*b* (Å)	*c* (Å)
A.S.T.M.	10.330	6.010	4.692
$LiFePO_4$/C	10.328	6.012	4.693
$LiFePO_4$/MWCNT/C	10.271	5.969	4.688
Co doped $LiFePO_4$/C	10.283	5.989	4.679

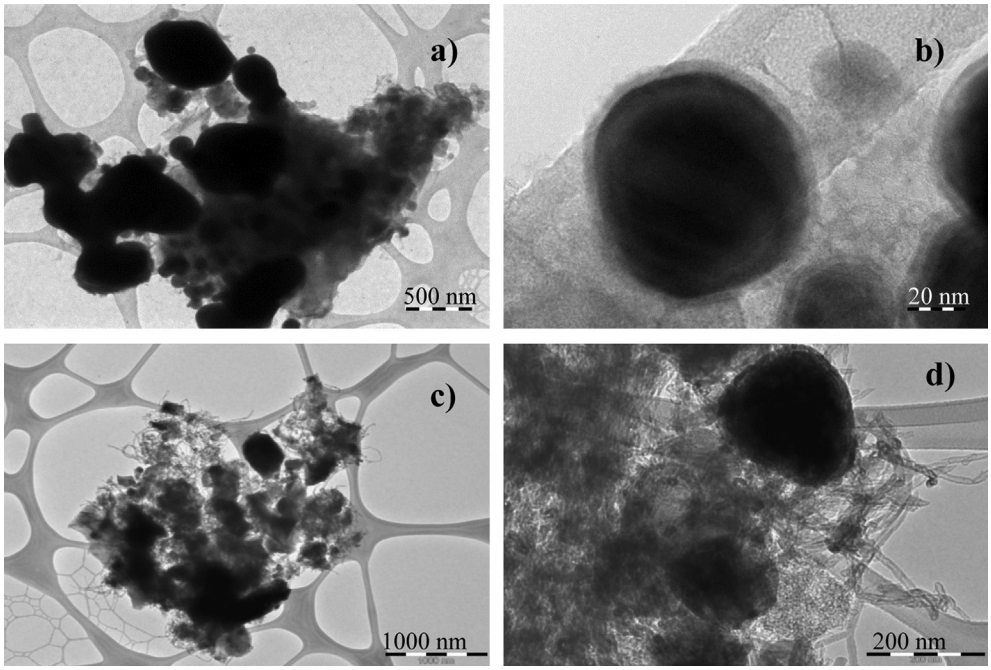

Fig. 2. TEM images of $LiFePO_4$/C particles (a) and (b) at two different magnifications and TEM images of $LiFePO_4$/MWCNT/C particles at two different magnifications (c) and (d).

3. Results and discussion

3.1. XRD analysis

The XRD patterns of prepared $LiFePO_4$/C, $LiFePO_4$/MWCNT/C and cobalt doped $LiFePO_4$/C samples are shown in Fig. 1. The main phase of all prepared materials can be indexed as *Pnma* orthorhombic structure of synthetic triphylite $LiFePO_4$ structure. It was found that minor amounts of impurity phases like Li_3PO_4, magnetite Fe_3O_4 and barringerite Fe_2P were present. The diffraction peak intensity of $LiFePO_4$/C/MWCNT is higher than that of $LiFePO_4$/C but very similar to that of 1%Co $LiFePO_4$/C. The results prove that the modified solid state synthesis method can reduce the synthesis temperature and reaction time compared with the ordinary method. The grain size after Co and MWCNT addition was same or very similar to grains size of pure $LiFePO_4$ cathode material. The X-ray pattern of our samples is in quantitative agreement with prior works and the lattice parameters *a*, *b*, *c* (Table 1) deduced from the analysis of the diffraction pattern using a least-square fit for the *Pnma* orthorhombic space group are found in quantitative agreement with X-ray Powder Diffraction Data File, published by A.S.T.M. (American Society for Testing Materials).

3.2. TEM analysis

Fig. 2a and b shows the TEM images of the pure $LiFePO_4$/C sample without doping or additional support. It is possible to see the coated nanoparticles of the active material fixed in a carbon matrix. High resolution images indicate the coating the crystalline

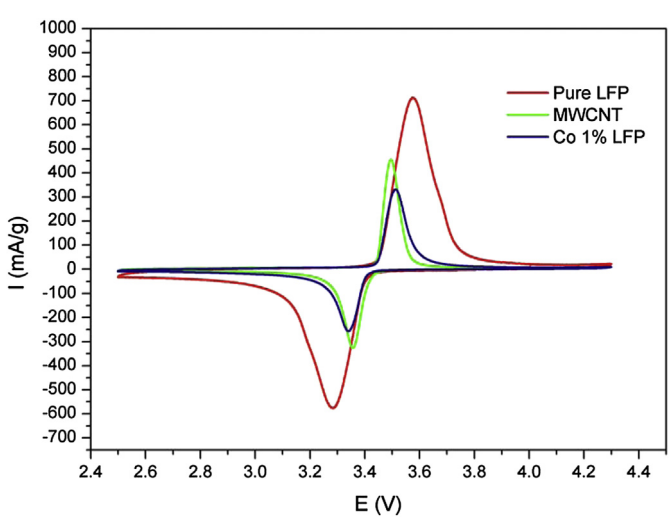

Fig. 3. Cyclic voltammograms of pure $LiFePO_4$/C, $LiFePO_4$/C/MWCNT and Co doped $LiFePO_4$/C.

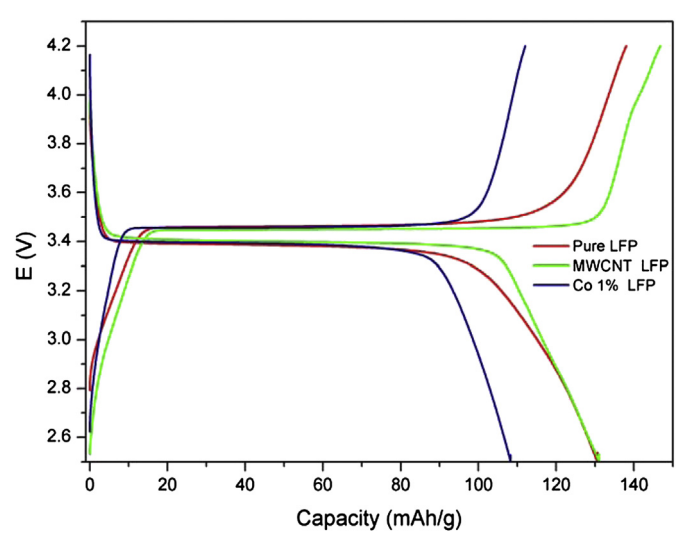

Fig. 4. Charge–discharge profiles of prepared samples measured at C/5 charge and C/5 discharge rate.

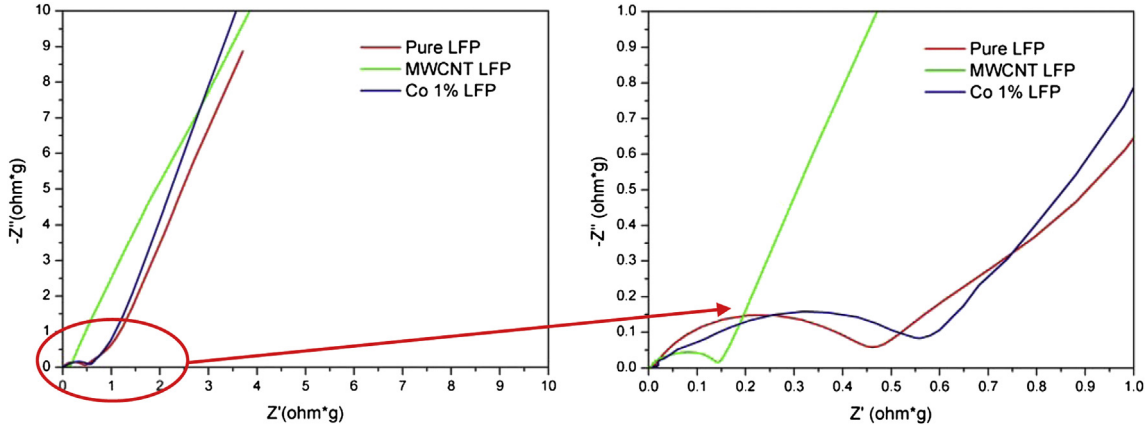

Fig. 5. EIS Nyquist plots measured on $LiFePO_4$/C, $LiFePO_4$/MWCNT/C and cobalt doped $LiFePO_4$/C.

active material particles with carbon. Fig. 2c and d shows a low and a high-magnification image of the $LiFePO_4$/MWCNT/C sample. It is possible to see carbon coated nanoparticles fixed in mixed MWCNT and carbon matrix. The multiwall carbon nanotubes provide highly conductive inter-particle connection between carbon coated core-shell structured particles and thus improves the electronic conductivity. The diameter of $LiFePO_4$ particles varies from 40 nm to 200 nm. Our $LiFePO_4$/C samples are characterized by a complex structure, nanometre sized, formed by single particles, strings and clusters.

3.3. Electrochemical characterization

Fig. 3 shows the cyclic voltammograms of $LiFePO_4$/C, $LiFePO_4$/MWCNT/C and cobalt doped $LiFePO_4$/C measured at a sweep rate 0.1 mV s^{-1}. The tenth cycle at all samples is shown and no significant changes in CV curves during the cycling indicate a good cyclability of all materials. In all samples, single cathodic and anodic peak is present and it illustrates one electron exchange reaction during the $LiFePO_4$ to $FePO_4$ transformation. All currents were calculated per weight of active $LiFePO_4$ material. Pure material has the highest specific anodic and cathodic current, nevertheless MWCNT supported and Co doped materials have a slightly higher anodic peak potential. Also the sintering temperature has a considerable effect on the properties of final $LiFePO_4$ products affecting not only the purity of $LiFePO_4$ particles, but also the discharge capacity of the material [18,19]. Therefore, a moderate temperature is very important. In general, the appropriate sintering temperature range is 650–750 °C.

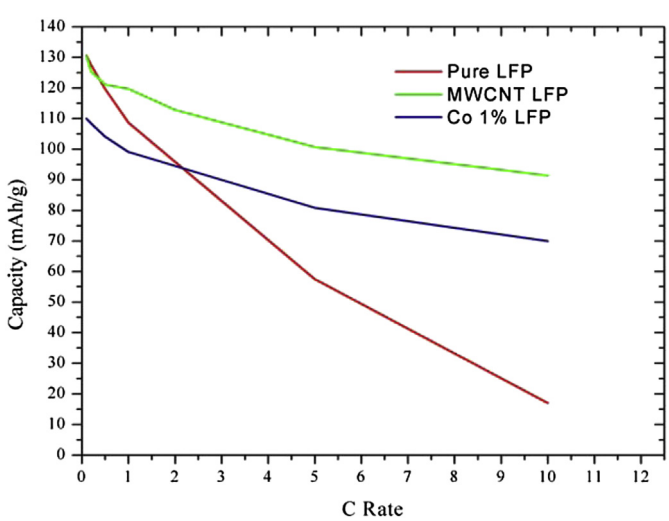

Fig. 6. Rate capability of $LiFePO_4$/C, $LiFePO_4$/MWCNT/C and cobalt doped $LiFePO_4$ at rate C/5.

Fig. 4 shows the charge–discharge profiles of pure, MWCNT supported and Co doped $LiFePO_4$/C composite material measured at C/5 charge and discharge rates. All samples have a flat plateau at 3.4 V across a long capacity range. There is a slight difference in the charge and discharge plateau voltages that can be attributed to the polarisation of electrode due to impurity phases.

The electrochemical impedance spectroscopy measurements represented as Nyquist plot are on Fig. 5. Typical characteristics for Li-ion cells were obtained. A depressed semicircle in high frequency region gives information about electrolyte resistance, single particle insulating layer and charge transfer resistance [20]. The straight line in the low frequency region describes solid state diffusion of Li^+ ions into the particle material. According to the impedance results pure $LiFePO_4$/C and MWCNT supported $LiFePO_4$/C are almost the same regarding charge transfer resistance and very similar in diffusion region. The sample with MWCNT support exhibits three times lower charge transfer resistance. Porous microstructure and large surface area of MWCNT may provide a lot of transport passage for lithium-ion, which also may increase the lithium-ion diffusion. Among the three samples, the sample with MWCNT support showed the lowest resistance, suggesting that the MWCNT coating improved the conductivity of the battery. The small impedance of $LiFePO_4$/C/MWCNT sample can be attributed to the higher electronic conductivity resulted from the MWCNT/$LiFePO_4$ network.

Fig. 6 shows the rate capability of $LiFePO_4$/C, $LiFePO_4$/MWCNT/C and cobalt doped $LiFePO_4$/C composite materials. The measurement was made with a fixed charge rate of C/5 and varying subsequent discharge rates from C/10 to 10C. The pure $LiFePO_4$/C sample exhibits a significant discharge capacity drop from 130 mA h g^{-1} at C/10 to 20 mA h g^{-1} at 10C. The $LiFePO_4$/MWCNT/C sample and cobalt doped $LiFePO_4$/C demonstrate excellent rate capabilities with different capacities but with the same amount of capacity fade out. All capacities are related to the content of active $LiFePO_4$ material.

4. Conclusions

Nanostructured $LiFePO_4$/C composite electrode materials that can be improved in two different ways have been synthesized by a temperature assisted solid state synthesis using glycine as a carbon

precursor for particle coating. An addition of a highly conductive MWCNT support instead of Super P during the synthesis and doping by 1% of cobalt were the techniques to successfully improve the performance of electrode materials in the high discharge rate region. The basic $LiFePO_4$/C material exhibits capacity of 130 mA h g^{-1} at C/5 and 20 mA h g^{-1} at 10C rate, cobalt doped sample exhibits capacity of 110 mA h g^{-1} at C/5 and 70 mA h g^{-1} at 10C rate and $LiFePO_4$/C/MWCNT material has capacity of 130 mA h g^{-1} at C/5 and 90 mA h g^{-1} at 10C. $LiFePO_4$/C/MWCNT and Co doped $LiFePO_4$/C materials have almost the same slope of rate capability curve but $LiFePO_4$/C/MWCNT sample exhibits higher high-rate capacity. An addition of MWCNT and doping by Co ions offers an easy way to improve the performance of samples produced by glycine assisted solid state synthesis.

Acknowledgements

This work was supported by Czech Science Foundation, No. P102/10/2091, Center of Research and Utilization of Renewable Energy Sources, No. CZ.1.05/2.1.00/01.0014, and project CZ.1.07/2.3.00/30.0039 of Brno University of Technology.

References

[1] J.W. Fergus, J. Power Sources 195 (2010) 939–954.
[2] v. Schalkwijk, Walter, Scrosati, in: W.A. van Schalkwijk, B. Scrosati (Eds.), Advances in Lithium-Ion Batteries, Springer, 2002, p. 524.
[3] A.K. Padhi, K.S. Nanjundaswamy, J.B. Goodenough, J. Electrochem. Soc. 144 (1997) 1188–1194.
[4] Y. Wang, P. He, H. Zhou, Energy Environ. Sci. 4 (2011) 805–817.
[5] C. Wang, J. Hong, Electrochem. Solid-State Lett. 10 (2007) A65.
[6] L.F. Nazar, G. Goward, F. Leroux, M. Duncan, H. Huang, T. Kerr, J. Gaubicher, Int. J. Inorg. Mater. 3 (2001) 191–200.
[7] R. Pitchai, V. Thavasi, S.G. Mhaisalkar, S. Ramakrishna, J. Mater. Chem. 21 (2011) 11040–11051.
[8] N. Kalaiselvi, A. Manthiram, J. Power Sources 195 (2010) 2894–2899.
[9] E.M. Bauer, C. Bellitto, G. Righini, M. Pasquali, A. Dell'Era, P.P. Prosini, J. Power Sources 146 (2005) 544–549.
[10] F.-Y. Kang, J. Ma, B.-h. Li, New Carbon Mater. 26 (2011) 161–170.
[11] L. Wang, Z. Tang, L. Ma, X. Zhang, Electrochem. Commun. 13 (2011) 1233–1235.
[12] R.-r. Zhao, I.M. Hung, Y.-T. Li, H.-y. Chen, C.-P. Lin, J. Alloys Compd. 513 (2012) 282–288.
[13] T. Muraliganth, A. Manthiram, J. Phys. Chem. C 114 (2010) 15530–15540.
[14] N. Penazzi, M. Arrabito, M. Piana, S. Bodoardo, S. Panero, I. Amadei, J. Eur. Ceram. Soc. 24 (2004) 1381–1384.
[15] C. Li, N. Hua, C. Wang, X. Kang, W. Tuerdi, Y. Han, J. Alloys Compd. 509 (2011) 1897–1900.
[16] Y. Ge, X. Yan, J. Liu, X. Zhang, J. Wang, X. He, R. Wang, H. Xie, Electrochim. Acta 55 (2010) 5886–5890.
[17] M.R. Roberts, G. Vitins, J.R. Owen, J. Power Sources 179 (2008) 754–762.
[18] Z.-y. Chen, H.-l. Zhu, S. Ji, R. Fakir, V. Linkov, Solid State Ionics 179 (2008) 1810–1815.
[19] A. Yamada, S.C. Chung, K. Hinokuma, J. Electrochem. Soc. 148 (2001) A224–A229.
[20] N. Bonanos, B.C.H. Steele, E.P. Butler, Applications of impedance spectroscopy, in: Impedance Spectroscopy, John Wiley & Sons, Inc., 2005, pp. 205–537.